Original Article

MOLECULAR METABOLISM

Pharmacologic inhibition of ketohexokinase prevents fructose-induced metabolic dysfunction

Jemy A. Gutierrez [1,6], Wei Liu [1,6], Sylvie Perez [1], Gang Xing [1], Gabriele Sonnenberg [1], Kou Kou [1], Matt Blatnik [2], Richard Allen [4], Yan Weng [5], Nicholas B. Vera [1], Kristin Chidsey [3], Arthur Bergman [5], Veena Somayaji [3], Collin Crowley [1], Michelle F. Clasquin [1], Anu Nigam [1], Melissa A. Fulham [1], Derek M. Erion [1], Trenton T. Ross [1], William P. Esler [1], Thomas V. Magee [1], Jeffrey A. Pfefferkorn [1], Kendra K. Bence [1], Morris J. Birnbaum [1], Gregory J. Tesz [1,*]

ABSTRACT

Objective: Recent studies suggest that excess dietary fructose contributes to metabolic dysfunction by promoting insulin resistance, de novo lipogenesis (DNL), and hepatic steatosis, thereby increasing the risk of obesity, type 2 diabetes (T2D), non-alcoholic steatohepatitis (NASH), and related comorbidities. Whether this metabolic dysfunction is driven by the excess dietary calories contained in fructose or whether fructose catabolism itself is uniquely pathogenic remains controversial. We sought to test whether a small molecule inhibitor of the primary fructose metabolizing enzyme ketohexokinase (KHK) can ameliorate the metabolic effects of fructose.

Methods: The KHK inhibitor PF-06835919 was used to block fructose metabolism in primary hepatocytes and Sprague Dawley rats fed either a high-fructose diet (30% fructose kcal/g) or a diet reflecting the average macronutrient dietary content of an American diet (AD) (7.5% fructose kcal/g). The effects of fructose consumption and KHK inhibition on hepatic steatosis, insulin resistance, and hyperlipidemia were evaluated, along with the activation of DNL and the enzymes that regulate lipid synthesis. A metabolomic analysis was performed to confirm KHK inhibition and understand metabolite changes in response to fructose metabolism in vitro and in vivo. Additionally, the effects of administering a single ascending dose of PF-06835919 on fructose metabolism markers in healthy human study participants were assessed in a randomized placebo-controlled phase 1 study.

Results: Inhibition of KHK in rats prevented hyperinsulinemia and hypertriglyceridemia from fructose feeding. Supraphysiologic levels of dietary fructose were not necessary to cause metabolic dysfunction as rats fed the American diet developed hyperinsulinemia, hypertriglyceridemia, and hepatic steatosis, which were all reversed by KHK inhibition. Reversal of the metabolic effects of fructose coincided with reductions in DNL and inactivation of the lipogenic transcription factor carbohydrate response element-binding protein (ChREBP). We report that administering single oral doses of PF-06835919 was safe and well tolerated in healthy study participants and dose-dependently increased plasma fructose indicative of KHK inhibition.

Conclusions: Fructose consumption in rats promoted features of metabolic dysfunction seen in metabolic diseases such as T2D and NASH, including insulin resistance, hypertriglyceridemia, and hepatic steatosis, which were reversed by KHK inhibition.

Keywords Fructose; KHK; Insulin resistance; NAFLD; Metabolic disease

1. INTRODUCTION

Fructose has become a major ingredient in processed foods due to its perceived sweetness, humectant properties, and low cost. Due to these properties, increased consumption of highly processed foods has led to a concomitant increase in fructose consumption. Fructose is typically added to foods as table sugar, a fructose/glucose disaccharide, or high-fructose corn syrup (typically ~55% fructose and 45% glucose). In the US, sugar now accounts for greater than 10% of consumed calories with ~13% of the population consuming in excess of 25% of daily calories as added sugar [1]. Numerous studies have demonstrated an association between sugar consumption and obesity

[1]Internal Medicine Research Unit, Pfizer Worldwide Research, Development, and Medical, Cambridge, MA 02139 USA [2]Early Clinical Development, Pfizer Worldwide Research, Development, and Medical, Groton, CT 06340 USA [3]Early Clinical Development, Pfizer Worldwide Research, Development, and Medical, Cambridge, MA 02139 USA [4]Quantitative Systems Pharmacology, Pfizer Worldwide Research, Development, and Medical, Cambridge, MA 02139 USA [5]Clinical Pharmacology, Pfizer Worldwide Research, Development, and Medical, Cambridge, MA 02139 USA

[6] These authors contributed equally to this study.

*Corresponding author. Pfizer Worldwide Research, Development, and Medical, 1 Portland Street Cambridge, MA 02139, USA. Tel.: 617-551-3546. E-mail: gregory.tesz@pfizer.com (G.J. Tesz).

Received December 23, 2020 • Revision received February 21, 2021 • Accepted February 23, 2021 • Available online 3 March 2021

https://doi.org/10.1016/j.molmet.2021.101196

Abbreviations

T2D	type 2 diabetes
NAFLD	non-alcoholic fatty liver disease
NASH	non-alcoholic steatohepatitis
KHK	ketohexokinase
DNL	de novo lipogenesis
AD	American diet
ChREBP	carbohydrate response element-binding protein
ApoC3	apolipoprotein C3
F1P	fructose-1-phosphate
ATP	adenosine triphosphate
TCA	tricarboxylic acid
DHAP	dihydroxyacetone phosphate
G6P	glucose-6-phosphate
Pklr	pyruvate kinase
Acc1	acetyl-CoA carboxylase 1
Acly	ATP-citrate synthase
Fasn	fatty acid synthase
AldoB	aldolase B
Tk	triose kinase
Glut5	solute carrier family 2-facilitated glucose transporter member 5
D_2O	deuterium oxide
HFI	hereditary fructose intolerance
PPD	paraphenylenediamine
CRU	Clinical Research Unit
HPLC	high-performance liquid chromatography
UPLC	ultra-performance liquid chromatography
GC	gas chromatograph
LC-MS/MS	liquid chromatography with tandem mass spectrometry
CAD	charged aerosol detection
CO_2	carbon dioxide
EDTA	ethylenediaminetetraacetic acid
DMSO	dimethyl sulfoxide
PBS	phosphate-buffered saline
TBS	Tris-buffered saline
TBST	Tris-buffered saline with 0.1% Tween 20
AUC	area under the curve
BID	two doses daily
DMEM	Dulbecco's Modified Eagle Medium
FBS	fetal bovine serum
MRM	multiple reaction monitoring
FAME	fatty acid methyl esters
TG	triglyceride
FA	fatty acid
BMI	body mass index

[2,3], type 2 diabetes (T2D) [2,3], cardiovascular risk factors [4–6], non-alcoholic fatty liver disease (NAFLD) [7–10], and non-alcoholic steatohepatitis (NASH) [11]. While the World Health Organization and American Heart Association recommend limiting sugar consumption to <5% of daily calories [12,13], implementing these guidelines on a global scale remains challenging.

Whether sugar promotes metabolic dysfunction due to excess dietary calories hidden in processed foods or whether the metabolism of fructose within sugar is uniquely pathogenic remains controversial. While some studies suggest that overconsumption of fructose is pathogenic due to excess caloric intake [14], more recent calorically matched studies demonstrate that fructose overconsumption promotes negative metabolic adaptations in humans such as hyperlipidemia, insulin resistance, steatosis, increased de novo lipogenesis (DNL), cardiovascular risk factors, and visceral adiposity to a greater extent than glucose overconsumption [15–17]. In a short-term study, 9 days of fructose feeding increased liver fat and DNL in human subjects [18]. In another study with multiple dose levels of fructose, ingestion of carbohydrates increased plasma triglycerides (TGs), uric acid, and apolipoprotein C3 (ApoC3) dose-responsively [19]. Short-term fructose restriction in children improved insulin sensitivity [20], decreased hepatic steatosis [18], and reduced ApoC3 and other cardiovascular risk factors [21], further supporting the causative role of fructose consumption in driving metabolic disease in humans.

The first committed step of fructose metabolism is its phosphorylation by ketohexokinase (KHK), expressed as two distinct enzyme isoforms, KHK-A and KHK-C [22]. KHK-C has a greater affinity and capacity for fructose phosphorylation relative to KHK-A. Expression of KHK-C is limited to the primary fructose metabolism sites, including the liver, kidney, and intestine, while KHK-A is ubiquitous at low levels [23]. KHK is essential for fructose metabolism as humans with loss-of-function KHK mutations and KHK-null mice fail to metabolize fructose, leading to the accumulation of fructose in plasma and urinary excretion [24–26]. Additionally, genetic deletion of KHK or knockdown with small interfering RNA protects mice from the deleterious metabolic effects of fructose, including obesity, insulin resistance, steatosis, hyperlipidemia, and hepatic inflammation, supporting therapeutic targeting of KHK as a method of mitigating metabolic diseases including NAFLD/NASH, T2D, and cardiovascular disease [26–29].

PF-06835919 was previously demonstrated to be a highly selective inhibitor of KHK-A/C by in vitro selectivity assays and no development-limiting findings were observed in rat and dog toxicology studies [30]. In this report, we demonstrate that the small molecule KHK-A/C inhibitor PF-06835919 reverses metabolic dysfunction caused by fructose consumption in rats, including hyperlipidemia, hepatic steatosis, and insulin resistance. Importantly, although these metabolic syndrome features are normally studied in rats fed fructose at supra-physiologic levels, we found that they also occur in rats fed a diet similar in macronutrient composition to the typical American diet (AD) and can be reversed by KHK inhibition. We demonstrate that PF-06835919 inhibits fructose metabolism in humans, highlighting this compound's potential utility in treating human metabolic diseases.

2. MATERIALS AND METHODS

2.1. KHK inhibitor

PF-06835919 was discovered and optimized as described by Futatsugi et al. [30]. For in vitro studies, PF-06835919 was freshly prepared in dimethyl sulfoxide (DMSO) (Sigma-Aldrich). For in vivo studies, PF-06835919 was formulated in 0.5% methylcellulose (Sigma-Aldrich) at the indicated dose as a 10 mL/kg suspension. PF-06835919 was administered as two doses daily (BID) between 7–8 AM and 3–4 PM

throughout all of the studies. Methylcellulose vehicle and PF-06835919 were prepared weekly.

2.2. Culture of primary hepatocytes

Fresh rat hepatocytes from non-fasted Sprague Dawley rats were isolated by Biomere (Worcester, MA, USA) and counted immediately upon arrival. Hepatocytes were plated in low glucose Dulbecco's Modified Eagle Medium (DMEM) containing 10% fetal bovine serum (FBS), 1 nM insulin, 0.1 μM dexamethasone, and 1x penicillin-streptomycin. Cryopreserved human hepatocytes (Corning Life Science) were thawed in prewarmed thawing media and plated according to the manufacturer's instructions (BioIVT).

2.2.1. Inhibition of KHK activity in primary human and rat hepatocytes

Human hepatocytes were seeded on a 96-well collagen-coated plate at 50,000 cells/well using plating media (BioIVT). After a 4-hr incubation, the media was aspirated, and the cells were treated with Matrigel matrix and incubated overnight. The following morning, the media was replaced with William's E media prior to compound treatment. Rat hepatocytes were plated identically in 96-well collagen-coated plates at 70,000 cells/well.

Serial dilution of PF-06835919 was prepared in DMSO and further diluted to 1:10 in deionized water prior to treating the plated hepatocytes. After a 30-min preincubation with inhibitor, 10 mM [$^{13}C_6$]-D-fructose (Sigma-Aldrich) was added, and the reaction was allowed to proceed for 20 min for human hepatocytes and 45 min for fresh rat hepatocytes. The medium was removed and the reaction was quenched with cold lysis buffer (80% methanol, 20% water, 3 μM [$^{13}C_5$]-D-xylitol [Omicron Biochemicals]). The hepatocytes were lysed on a plate shaker for 15 min. The well contents were transferred and stored at −80 °C for liquid chromatography with tandem mass spectrometry (LC-MS/MS) analysis of the fructose-1-phosphate (F1P) product (see Section 2.4).

2.2.2. Fructose metabolism studies in primary rat hepatocytes

Rat hepatocytes were plated in 12-well collagen-coated plates at 660,000 cells/well and incubated for 4 hrs at 37 °C with 5% CO_2 William's E media. After a 4-hr incubation, the cells were washed with phosphate-buffered saline (PBS) and the media was changed. The hepatocytes were preincubated with 30 μM PF-06835919 or DMSO prior to adding 10 mM [$^{13}C_6$]-fructose (Sigma-Aldrich). The hepatocytes were harvested after the appropriate incubation period on ice with an ice-cold PBS wash followed by lysis in ice-cold 80% methanol/20% distilled-deionized water. The plates were stored at −80 °C until subsequent analysis. The incorporation of $^{13}C_6$ carbons into glycolytic and tricarboxylic acid (TCA) metabolites was determined using the liquid chromatography-high resolution mass spectrometry method described by Meissen et al. [31].

2.2.3. ChREBP translocation assay in primary hepatocytes

Rat hepatocytes were plated in 96-well collagen-coated plates at 50,000 cells/well and incubated for 4 hrs at 37 °C with 5% CO_2. After 4 hrs, the cells were washed and then incubated in M199 media containing 1 nM insulin and 0.1 μM dexamethasone overnight. The following day, carbohydrate concentrations were adjusted to 5 mM glucose +/− 10 mM fructose or 25 mM glucose, and 30 μM PF-06835919 or DMSO was added for 24 hrs. The hepatocytes were fixed with 4% paraformaldehyde in PBS and permeabilized in PBS containing 0.1% Triton X-100. The cells were immune-labeled with ChREBP (M−300) antibody (Santa Cruz) at 1:250 dilution overnight at 4 °C and goat anti-rabbit IgG (H + L) secondary antibody with Alexa Fluor 594 conjugate (Invitrogen A-11037) at 1:1000 for 1 hr. ChREBP nuclear localization was measured and images were acquired on Operetta High-Content Imaging System.

2.2.4. Gene expression in rat hepatocytes

Rat hepatocytes were plated in 6-well collagen-coated plates at 1.3 million cells/well and incubated for 4 hrs at 37 °C with 5% CO_2. Hepatocyte health was assessed, and the cells were washed twice with PBS to remove dead cells and media identical to the plating media was added. Some wells were also supplemented with 10 mM fructose +/− PF-06835919. After 18 hrs, the cells were washed twice with PBS and RNA was isolated from the cells using a Qiagen RNeasy RNA isolation kit. cDNA was amplified using iScript cDNA synthesis kit (Bio-Rad) and the gene expression was determined using an Applied Biosystems Quant Studio 7 flex (Thermo Fisher Scientific).

2.3. Rat studies

All the animal procedures were conducted in accordance with regulations and guidelines established by the National Institutes of Health's Guidelines for the Care and Use of Laboratory Animals and were reviewed and approved by Pfizer's Institutional Animal Care and Use Committee. Male Sprague Dawley rats weighing ∼200 g (Charles River) were acclimated in a reverse 12-hr day/night cycle. The rats were fed either standard chow, PicoLab Rodent Diet 20 (5053, LabDiets), a high-fructose diet containing 30% fructose provided as 60% sucrose (D13032001, Research Diets), or an American diet containing 35% kcal fat and 14% sucrose (D16032201, Research Diets) ad libitum. The rats were randomized by body weight into appropriate treatment groups for every study.

2.3.1. Dietary fructose study

Acclimated rats were administered PF-06835919 (3, 10, or 30 mg/kg orally twice per day) on day 1 of the study and immediately switched to fructose chow (D13032001). Body weights were measured twice per week to adjust dosing volumes. Fasted plasma was collected after an 8-hr fast in K2-ethylenediaminetetraacetic acid (EDTA) tubes 5 days prior to the study's start and then weekly after the start of dosing. On day 16, PF-06835919 and fructose was measured in plasma over a 24-hr period. On day 37, 24-h food consumption was determined by measuring food weight. Urine was also collected over 24 hrs on day 37 to determine fructose levels. The rats were sacrificed in two equal cohorts after 48 or 49 days of treatment in the fed state by carbon dioxide (CO_2) asphyxiation. The terminal blood was collected using a cardiac stick and exsanguination, and the livers were promptly removed and slices for histological analysis were collected. Histological sections were prepared and stained for lipid using osmium paraphenylenediamine (PPD) and mounted as described by Shirai et al. [32]. Liver sections were scanned on a Leica Systems Aperio AT2 whole digital slide scanner at a 20x objective setting. The remaining tissue was flash frozen in liquid nitrogen. Plasma triglycerides were measured by summation of triglyceride species detected using the lipidomic method (see Section 2.4.3). Plasma insulin and adiponectin were measured using the Meso Scale Discovery insulin and adiponectin assay kits (Meso Scale Diagnostics) and analyzed using a SECTOR Imager 6000 (Meso Scale Diagnostics).

2.3.2. In vivo measurement of DNL

Sprague Dawley rats were on chow or high-fructose diets for 2 weeks and then treated orally with either vehicle or PF-06835919 BID at 3,

10, and 30 mg/kg/day. On day 9 of the study, the rats were orally administered 100% deuterium oxide (D_2O) (equivalent to 5% of body water) and then maintained on 5% D_2O for 5 additional days. The rats were sacrificed in the fed state by CO_2 asphyxiation and their cardiac blood was collected in K2-EDTA tubes according to the manufacturer's protocol for plasma isolation. ^{2}H-palmitate was measured as fatty acid methyl esters by gas chromatography–mass spectroscopy as described in Section 2.4.4.

2.3.3. American diet study

Sprague Dawley rats were randomized into 5 dose groups and fed either standard rodent chow (Pico 20, LabDiet) or a custom "American diet" (AD, D16032201, Research Diets) (35% kcal fat and 14% sucrose/7% fructose) ad libitum for 9 weeks in total. At week 8, the animals were orally administered either PF-06835919 (6, 20, or 60 mg/kg/day) or vehicle (0.5% methylcellulose) BID. The rats were euthanized by CO_2 asphyxiation in the fed state. The terminal blood was collected by a cardiac stick and exsanguination, and the livers were promptly removed and flash frozen. Plasma was separated from whole blood collected in K2-EDTA tubes according to the manufacturer's protocol. Plasma triglycerides, free fatty acids, and total cholesterol were measured using Advia XPT (Siemens). Plasma ApoC3 was determined by enzyme-linked immunosorbent assays (Thermo Fisher Scientific). Plasma insulin was measured as described in Section 2.3.1.

2.3.4. Determination of PF-06835919 potency in rat liver, kidney, and intestines

Male Sprague Dawley rats (~200 g body weight) containing a jugular vein cannula (Charles River) were acclimated on standard chow for one week prior to the study. Three separate experiments were conducted using doses of PF-06835919 ranging from 0.1 mg/kg to 500 mg/kg. The rats were fasted overnight for 16 hrs prior to the study. The rats were orally administered a single dose of PF-06835919 1 hr prior to jugular vein administration of a 10 mL/kg bolus of fructose, 500 mg/kg over 20 s. The rats were sacrificed by decapitation 2 mins later and their livers and kidneys were promptly removed and freeze-clamped in liquid nitrogen. Blood was collected in K2-EDTA tubes for plasma isolation. All the samples were stored at −80 °C until processing. The plasma and liver samples were sent to Pfizer's Pharmacokinetics, Dynamics, and Metabolism (PDM) group in Groton, CT, to determine the PF-06835919 concentrations.

For intestinal determination of KHK inhibition, male rats fed standard chow were fasted overnight for 16 hr and then orally administered a single dose of PF-06835919 (30 mg/kg). One hour later, a fructose bolus (2 g/kg) was administered and the animals were anesthetized with Nembutal. A section of intestine proximal to the jejunum and ileum was removed 15 mins later, flushed with ice-cold PBS, and snap frozen in liquid nitrogen. The rats were sacrificed by exsanguination. Frozen liver, kidney, and intestinal tissue wrapped in aluminum foil was pulverized on a liquid nitrogen-cooled metal block. Approximately 100 mg of tissue was aliquoted into a 2 mL Lysing Matrix D tube (MP Biomedicals) precooled in liquid nitrogen and 1 mL of homogenization buffer (10 mM ammonium acetate and 10 mM EDTA, pH 8) containing 3 μM [$^{13}C_5$]-xylitol as an internal standard. The samples were lysed at 4 °C using a FastPrep 24 (MP Biomedicals) and cleared by centrifugation. Supernatant (125 μL) was transferred to a 1.5 mL tube containing 250 μL of mass spectroscopy-grade water and cleared again by centrifugation. Supernatant was transferred to a deep 96-well plate, sealed, and stored at −80 °C until analysis as described in Section 2.4.

2.3.5. Assessment of KHK inhibition on plasma glucose, fructose, and sorbitol

Overnight-fasted rats were orally administered a single dose of vehicle (0.5% methylcellulose) or PF-06835919. Two hours after PF-06835919 treatment, the rats were given a 50:50 solution of $^{12}C_6$ and $^{13}C_6$ fructose (Sigma-Aldrich) at 10 mL/kg dissolved by gavage. After administration of fructose, blood was collected at 15, 30, 60, and 120 mins via the tail vein in K2-EDTA tubes and the plasma was separated. The rats were sacrificed by CO_2 asphyxiation, and a terminal blood sample was collected via a cardiac stick 4 hrs after fructose administration. Plasma concentrations of fructose, glucose, and sorbitol were measured by liquid chromatography and mass spectrometry as described in Section 2.4.2.

2.3.6. Effects of KHK inhibition on urine fructose concentrations after fructose bolus

The rats were acclimated on standard chow for 1 week prior to the study. For 24-hr urine collection, the rats were housed in metabolic cages. The rats were orally administered PF-06835919 or vehicle (0.5% methylcellulose) BID. One hour after the initial dose, the rats were orally administered 2 g/kg of a 50:50 solution of $^{12}C_6$ and $^{13}C_6$ fructose. Eight hours after the initial dose of PF-06835919, the rats were administered a second dose. After a 24-hr urine collection, the animals were returned to their cages. Urine volume was measured and cleared of debris by centrifugation. The urine was frozen and stored at −80 °C until further analysis. Urine fructose was measured as described in Section 2.4.2.

2.4. Analysis of tissues and cells

2.4.1. LC-MS/MS analysis of fructose-1-phosphate from tissues

F1P was extracted from hepatocytes and tissue lysates prepared as described in Sections 2.2.1 and 2.3.4, respectively. F1P was quantified on a QTRAP 5500 mass spectrometer (Sciex) coupled with Acquity ultra-performance liquid chromatography (UPLC, Waters) following the multiple reaction monitoring (MRM) transition of 259 → 97 using the following tune settings: curtain gas, 35; collision gas, medium; ion spray voltage, −4500 V; temperature, 700 °C; ion source gas 1, 40; ion source gas 2, 60; declustering potential, −47; entrance potential, −13.75; collision energy, −20.9; and collision cell exit potential, −16.8.

The separation of F1P from other sugar phosphates was performed with a Shodex RSpak JJ 50 2D PEEK column (2 × 150 mm) with an isocratic flow of 10% acetonitrile, 90% water, and 20 mM triethyl ammonium acetate. [$^{13}C_5$]-xylitol (1 μM for hepatocytes and 3 μM for tissue lysate) was used to determine the relative concentration of F1P in each sample. Percent inhibition was determined for kidney and liver F1P changes in response to increasing doses of PF-06835919.

2.4.2. LC-MS/MS analysis of plasma and urine fructose, glucose, and sorbitol

Plasma fructose, glucose, and sorbitol were extracted using nine equivalents of extraction solution, 80% methanol, and 20% aqueous solution containing 10 mM ammonium acetate, 10 mM EDTA, and 3 μM internal standard [$^{13}C_5$]-xylitol, pH 8. The extracts were cleared by centrifugation at 4 °C. The supernatant was transferred and diluted with 2 equivalents mass spectrometry-grade water prior to injection. Urine samples were mixed in a 1:1 ratio with acetonitrile (100 μL each), vortexed, and left on ice for 5 min. The samples were cleared by centrifugation and the supernatant was saved. The residual pellets were washed with 100 μL of 1:1 methanol:water and combined with

the initial supernatant. The supernatant was dried and suspended in 200 μL of extraction buffer (80% methanol and 20% aqueous solution containing 10 mM ammonium acetate and 10 mM EDTA). The extracts then underwent three cycles of freeze/thaw/centrifugation and were further diluted to 1:400.

Sugar separation was achieved by hydrophilic interaction chromatography using Asahipak NH2P-50 4E columns (4.6 × 250 mm) under isocratic elution conditions with a 0.8 mL/min flow rate using 75% acetonitrile and 25% water containing 5 mM ammonium acetate, pH 9.2. The total method time was 20 mins with the separated sugars eluted within the first 11 mins on the chromatogram. QTRAP5500 mass spectrometry (Sciex) source parameters were as follows: curtain gas, 35; ion spray voltage, −4500 V; temperature, 650 °C; ion source gas 1, 65; ion source gas 2, 60. The following MRM transitions were used for quantitation: fructose/glucose 179 → 89, [$^{13}C_6$]-fructose/[$^{13}C_6$]-glucose 185 → 92, sorbitol 181 → 89; [$^{13}C_6$]-sorbitol 187 → 92, and [$^{13}C_5$]-xylitol 157 → 92.

Sugars were quantified against a matrix-matched calibration curve containing [$^{13}C_6$]-fructose, which was analyzed as the ratio to the [$^{13}C_5$]-xylitol internal standard. Peak integration was conducted using MultiQuant (Sciex).

2.4.3. Lipidomics analysis of plasma and tissue samples

Lipids were extracted from plasma by adding organic extraction solvent (dichloromethane:isopropanol:methanol, 25:10:65 v/v/v) containing 200 nM glyceryl triheptadecanoate, followed by vigorous shaking. Lipid extracts were LC-MS/MS analyzed using a QTRAP5500 mass spectrometer (Sciex) coupled to an Acquity UPLC (Waters). Lipid classes were separated by reversed-phase chromatography on an Acquity UPLC BEH300 C4 column (2.1 × 50 mm, 1.7 μm). Tripalmitate was analyzed using positive ion electrospray ionization in the MRM mode using the following conditions: curtain gas, 20; ion spray voltage, 5500 V; temperature, 500 °C; ion source gas 1, 70; ion source gas 2, 45; and transition, 824.8 → 551.5. Liquid chromatography peak integration was performed with MultiQuant software (Sciex) and quantified against the single glyceryl triheptadecanoate point.

2.4.4. Measurement of deuterium enrichment in plasma palmitate

Deuterium incorporation into plasma palmitate was measured via an Agilent 6890 gas chromatograph (GC) coupled to an Agilent 5973 MSD. Briefly, plasma lipids were extracted using Bligh and Dyer's method [33], followed by saponification and trans-esterification to fatty acid methyl esters (FAME) with boron trifluoride/methanol [34]. FAME species were separated on an Agilent HP 5MS GC column (0.25 × 30 mm and 0.25 μm) using a thermal gradient and detected with the electron impact in the selected ion monitoring mode. Peak integration was performed with Agilent MassHunter software. DNL was quantified using Lee et al.'s method [35], assuming a plasma D_2O enrichment of 5%. Correction for natural abundance was calculated by subtracting experimentally derived values from unlabeled samples [36].

2.4.5. Extraction and analysis of hepatic triglycerides

Rat liver was homogenized and extracted using Folch's method and analyzed by high-performance liquid chromatography (HPLC) coupled with charged aerosol detection (CAD) [37]. Briefly, liver was homogenized with cold methanol, followed by chloroform extraction including 50 μM butylated hydroxytoluene. Following overnight storage at 20 °C, 2.8 mL of 1 M potassium chloride was added and the samples were vortexed and centrifuged. The bottom organic phase was dried under nitrogen and then resuspended in 500 μL of chloroform for solid phase extraction that was conducted as previously described [38]. The neutral lipid eluent was dried under nitrogen and resuspended in 98:2 isooctane:isopropanol prior to analysis on HPLC-CAD.

HPLC was performed using a Zorbax Eclipse rapid resolution (4.6 × 150 mm and 3.5 μm) cyanopropyl column (Agilent) with a 1000:1:2 isooctane:isopropanol:acetic acid 50:50 isooctane:methyl tert-butyl ether gradient. Hepatic triglycerides were calculated against a standard curve for a triglyceride standard mix composed of equimolar tripalmitate, trioleate, and trilinoleate.

2.4.6. Western blotting

Rat liver tissue was homogenized in RIPA lysis buffer containing protease and phosphatase inhibitors (Roche). The protein concentration was determined using Micro BCA (Pierce) according to the manufacturer's protocol. For all of the blots except acetyl-CoA carboxylase (ACC), 30 μg of protein was separated using a 4–12% Criterion XT gel (Bio-Rad). For ACC, 10 μg of protein was separated using a 3–8% tris-acetate Criterion XT gel (Bio-Rad). Protein was transferred using a Bio-Rad Western blotting transfer system at 100 V for 1 hr onto nitrocellulose membranes. The membranes were blocked using SuperBlock T20 Tris-buffered saline (TBS) blocking buffer. Primary antibody incubations were diluted as indicated in Supplemental Table 4 in Tris-buffered saline with 0.1% Tween 20 (TBST) with 3% non-fat dry milk except for the ACC antibody, which was incubated in 5% BSA in TBST overnight. The membranes were washed in TBST and incubated with the appropriate secondary antibody at the indicated dilutions (Supplemental Table 4) in TBST with 3% non-fat dry milk or 5% BSA for 1 hr. The membranes were incubated with enhanced chemiluminescence Western blotting substrate and bands were visualized using a Fujifilm LAS 4000 imager (Fujifilm) and Multi Gauge V3.2 software (Fujifilm).

2.5. Randomized phase 1 clinical study to assess administration of single oral doses of PF-06835919 to healthy human study participants

Clinical trial C1061001 (NCT02974374) was a phase 1 study with a primary objective to evaluate the safety and tolerability of single oral escalating doses of PF-06835919 administered in healthy adult study participants by measuring their vital signs, electrocardiogram, safety laboratory markers, and adverse events. The secondary objective was to evaluate the pharmacokinetics of PF-06835919 in human study participants. As an exploratory objective, the pharmacodynamic effect of PF-06835919 on plasma fructose was also evaluated. C1061001 was conducted in compliance with the ethical principles originating in or derived from the Declaration of Helsinki and with all International Council for Harmonization and Good Clinical Practice Guidelines. In addition, all the local regulatory requirements were followed, including those affording greater protection to the safety of the study participants. The study was managed by Pfizer (the sponsor) and conducted at a Pfizer Clinical Research Unit (CRU) in the US (New Haven, CT). All the participants provided informed consent. The final protocol and informed consent documentation were reviewed and approved by the Institutional Review Board at the investigational center participating in the study.

2.5.1. C1061001 study design

Healthy males and females of non-childbearing potential between the age of 18 and 55 years were eligible for participation in the study. Subjects with a known or suspected history of hereditary fructose intolerance (HFI) based on answers to an HFI questionnaire were

excluded. A total of 16 subjects were randomized into a sequential 2-cohort, 4-period, and double-blind (participants and care providers) cross-over study. A sample size of 8 subjects per cohort for a total of 16 subjects across the two cohorts for this single dose-escalating and 4-period cross-over study (6 active and 2 placebo) was chosen based on the need to minimize the first exposure to humans of a new chemical entity and the requirement to provide adequate safety and toleration information at each dose level. Randomization was carried out using random permuted blocks. The first subject visit occurred on October 19, 2016, and the last subject visit was on January 12, 2017. Enrollment stopped when the pharmacokinetic limit was reached. The subjects were screened by an investigator. A randomization schedule was provided by Pfizer to the investigator and the subjects were assigned to receive the study regimen corresponding to the randomization number. All the randomized subjects completed the study and none of the subjects discontinued from the study. Dose escalation could have been stopped if it was determined that the safety and/or tolerability limits were reached.

Eligible participants who met the entry criteria were admitted to the CRU three days prior to dosing for each study period and fed a low-fructose diet to lead into the study. PF-06835919 or placebo were administered on day 1 of each period with a $\geq$6 day interval between doses. PF-06835919 was administered at 10 mg, 30 mg, 100 mg, 200 mg, 400 mg, and 600 mg or placebo according to the randomization schedule. This design allowed for within- and between-subject assessment of safety, tolerability, and pharmacokinetic profiling. On the dosing day in each study period, the participants were administered PF-06835919 in the morning and then provided breakfast 20 mins later. Lunch and dinner were provided 5 and 10 hrs, respectively, after administration of PF-06835919. Each of the 3 meals on day 1 was supplemented with a 500 mL fructose-containing beverage to allow the assessment of pharmacologic KHK inhibition. Then 2 mL blood samples were collected for plasma separation at 0, 1.5, 3, 5, 6, 8, 10, 11, and 12 hrs after the administration of PF-06835919. Plasma fructose concentrations were measured by LC-MS/MS as described in Section 2.4.2, and the area under the curve (AUC) from 0 to 10 hr after administration of PF-06835919 was calculated.

2.5.2. Modeling KHK inhibition in healthy human study participants

We conservatively assumed equal exposure of compound in the plasma and liver. Out of the 4,000 parameter sets reported by Allen et al. [39], we identified 503 that captured the untreated observed response in this trial. These were further refined by fitting five baseline parameters of the model (determining the distribution volume of fructose and metabolism rate of fructose) to match this clinical cohort as closely as possible (but were constrained to stay within 25% of their original value to retain consistency with the broader set of reports considered by Allen et al. [39]. To match the treated groups, an IC_{50} equation was fit to predict the concentration of PF-06835919. To remove outliers and poor fits, the top 50% of fits were retained for analysis. The observed mean human pharmacokinetics of PF-06835919 were implemented in the model. The average inhibition over the C1061001 period is shown in Figure 6C. We also noted from the data that the absorption or clearance of fructose following the second or third fructose doses might have been upregulated. Allen et al.'s model was only compared to single doses of fructose. Hence, for completeness and to match the observed data as closely as possible, we phenomenologically modeled this effect by allowing the fructose absorption rate to be a function of time (hence upregulated at later time points).

2.6. Clinical and non-clinical statistical analyses

All the non-clinical statistical analyses were conducted as described in the figure legends using GraphPad PRISM version 8.0.2. Safety and tolerability data from clinical study C1061001 were summarized descriptively and are not reported herein. Fructose AUC was calculated using the linear trapezoidal rule. Raw fructose data and fructose AUC were summarized descriptively by dose and presented graphically.

3. RESULTS

3.1. PF-06835919 potently inhibited KHK and fructose metabolism

In vitro, PF-06835919 inhibited recombinant human and rat KHK-C (IC_{50} 27.6 nM and 207 nM respectively) and human KHK-A (IC_{50} = 172 nM) at physiologic adenosine triphosphate (ATP) concentrations [30]. Fructose is rapidly phosphorylated by KHK to form fructose-1-phosphate (F1P), which is subsequently converted into glycolytic metabolites (Figure 1A). PF-06835919 dose-dependently inhibited F1P in primary human (IC_{50} = 0.232 μM) and rat hepatocytes (IC_{50} = 2.801 μM) incubated with fructose (Figure 1B).

Catabolized fructose is rapidly incorporated into glycolytic and TCA metabolites [40,41]. To determine whether KHK inhibition reduced the incorporation of fructose carbons into these metabolites, rat hepatocytes were treated with [$^{13}C_6$]-fructose in the presence and absence of PF-06835919. Since the sole source of fructose was $^{13}C_6$ labeled, greater than 80% $^{13}C_6$ enrichment in F1P was detected in both DMSO- and PF-06835919-treated hepatocytes (Figure 1C). However, the total [$^{13}C_6$]-F1P peak was reduced by up to 12-fold with compound treatment, confirming KHK inhibition (Supplemental Figure 1A). KHK inhibition also reduced ^{13}C incorporation and total peak areas of glycolytic metabolites [$^{13}C_3$]-dihydroxyacetone phosphate (DHAP), [$^{13}C_3$]-pyruvate, [$^{13}C_3$]-lactate, [$^{13}C_3$]-glucose-6-phosphate (G6P), and [$^{13}C_6$]-G6P (Figure 1D—H and Supplemental Figure 1B-F). Similarly, enrichment of [$^{13}C_6$]-fructose carbons in the TCA intermediates malate and citrate was reduced in PF-06835919-treated hepatocytes compared to the DMSO control (Figure 1I,J) along with total [$^{13}C_3$]-malate and [$^{13}C_3$]-citrate peak areas (Supplemental Figure 1G and H). Together, the reduction of F1P production and incorporation of fructose into glycolytic and TCA metabolites confirmed that PF-06835919 effectively blocked fructose metabolism.

Notably, glycolytic intermediates, particularly G6P, promote fructose-mediated DNL by upregulating lipogenic enzymes through activating the transcription factor ChREBP [42,43]. As shown in Figure 1K,L, both 25 mM glucose and 5 mM glucose plus 10 mM fructose robustly increased the activity of ChREBP as measured by its redistribution to the nucleus in the rat hepatocytes. PF-06835919 prevented fructose-dependent but not glucose-dependent nuclear localization of ChREBP. Similarly, fructose increased the expression of the ChREBP target genes *Pklr*, *Acc1*, *Acly*, *Fasn*, and *AldoB*, which was blocked by KHK inhibition (Figure 1M).

3.2. PF-06835919 inhibited systemic fructose metabolism in rats

We next tested whether pharmacological inhibition of KHK with PF-06835919 could suppress the effects of fructose in vivo. Sprague Dawley rats were chosen for our studies due to the favorable pharmacokinetic properties of PF-06835919 in rats compared to mice (data not shown). Following an intravenous fructose bolus, PF-06835919 dose-dependently inhibited F1P formation in both the liver and kidney tissue of the rats (Figure 2A). Similarly, intestinal F1P was significantly reduced by PF-06835919 treatment 25 min after an oral fructose bolus (Figure 2B).

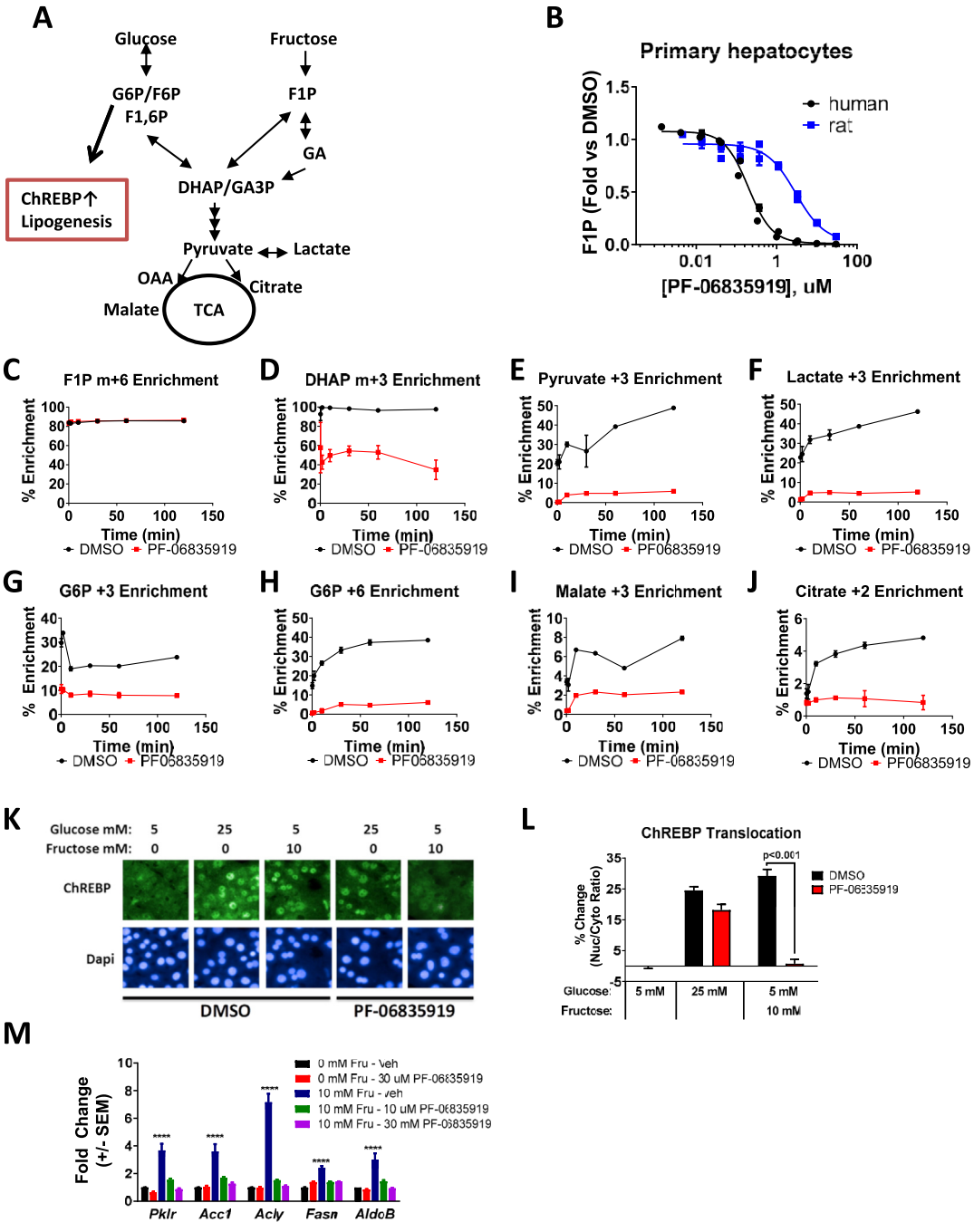

Figure 1: PF-06835919 blocked fructose metabolism and ChREBP activation in hepatocytes. (A) Graphical representation of fructose catabolism integrated in the glycolytic pathway. KHK phosphorylation of fructose leads to rapid accumulation of fructose-derived glycolytic metabolites, augmenting glycolysis and activating the lipogenic transcription factor ChREBP. (B) Inhibition of F1P generation in primary human and rat hepatocytes treated with PF-06835919 and fructose. Data points were calculated from 6 independent experiments for both human and rat hepatocytes. (C-H) Primary rat hepatocytes were incubated with 10 mM [$^{13}C_6$]-fructose +/− 30 μM PF-06835919 and the enrichment of fructose derived carbons in glycolytic metabolites was measured. Intracellular (C) [$^{13}C_6$]-F1P, (D) [$^{13}C_3$]-DHAP, (E) [$^{13}C_3$]-pyruvate, (F) [$^{13}C_3$]-lactate, (G) [$^{13}C_3$]-G6P, (H) [$^{13}C_6$]-G6P, (I) [$^{13}C_3$]-malate, and (J) [$^{13}C_2$]-citrate were measured from 3 biological replicates. The data are represented as mean +/− standard error of the mean. Representative images showing ChREBP cellular localization (K) from rat hepatocytes treated overnight with fructose or glucose +/− 30 μM PF-06835919. Green = ChREBP and blue = DAPI/nuclei. (L) Percent change in nuclear ChREBP compared to 5 mM of glucose and DMSO as measured by nuclear/cytoplasmic staining ratio (n = 5/group). (M) ChREBP target gene expression was measured in rat hepatocytes incubated overnight with 10 mM of fructose +/− PF-06835919. The data are mean +/− SEM calculated from the mean from four separate experiments with 3 biological replicates in each. Statistical significance was determined by two-way ANOVA and Bonferroni's test for multiple comparisons. ****$p < 0.0001$. Glucose-6-phosphate, G6P; fructose-6-phosphate, F6P; fructose-1,6-bisphosphate, F1,6P; fructose-1-phosphate, F1P; dihydroxyacetone phosphate, DHAP; glyceraldehyde, GA; glyceraldehyde-3-phosphate, GA3P; carbohydrate response element-binding protein, ChREBP; oxaloacetic acid, OAA; tricarboxylic acid, TCA; pyruvate kinase, *Pklr*; acetyl-CoA carboxylase 1, *Acc1*; ATP-citrate synthase, *Acly*; fatty acid synthase, *Fasn*; aldolase B, *AldoB*.

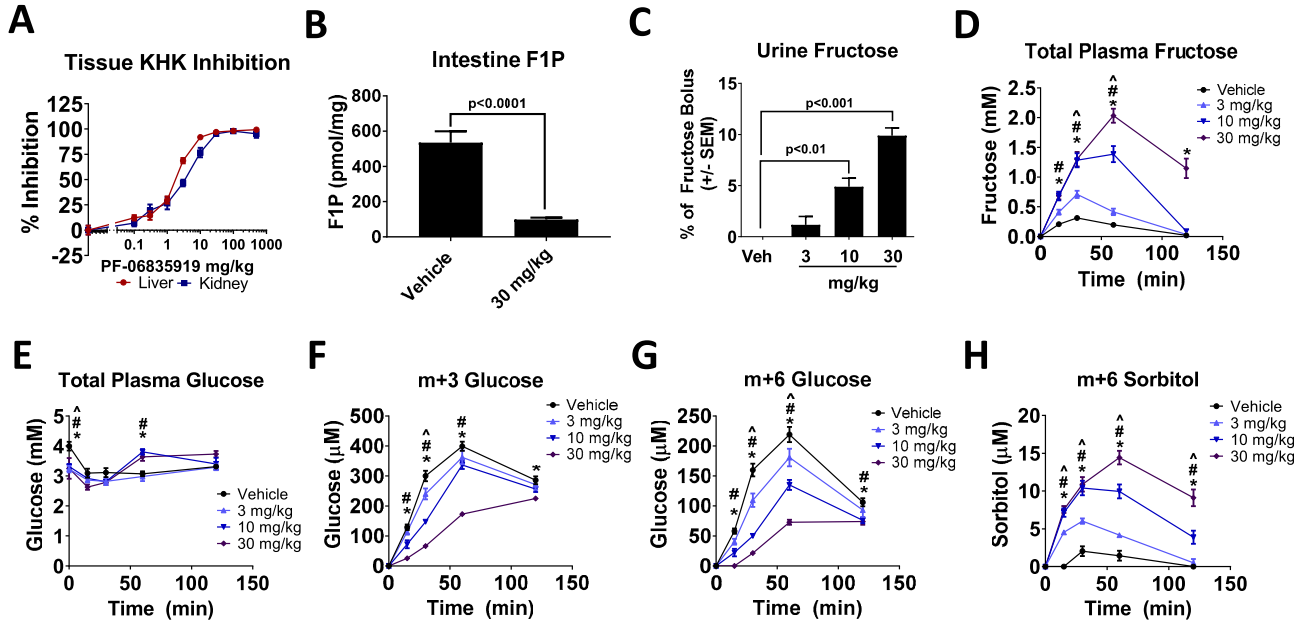

Figure 2: PF-06835919 inhibited fructose metabolism in the rats. (A) Hepatic and kidney fructose-1-phosphate (F1P) levels were measured in the rats administered vehicle and increasing doses of PF-06835919 after an acute intravenous fructose bolus (500 mg/kg). Percent inhibition was calculated from vehicle controls from three independent experiments and combined for analysis (n = 8–24/group). (B) Intestinal F1P measured in intestinal tissue samples from the vehicle- and PF-06835919-treated animals orally bolused with fructose (2 g/kg) (n = 6/group). Statistical significance determined by unpaired two-tailed t-test. (C) Urine fructose, (D) plasma fructose, (E) plasma glucose, and enrichment of fructose carbons in (F) [$^{13}C_3$]-glucose, (G) [$^{13}C_6$]-glucose, and (H) [$^{13}C_6$]-sorbitol were measured in the rats administered PF-06835919 (3, 10, and 30 mg/kg) after an oral bolus of a 2 mg/kg 50:50 mixture of $^{13}C_6/^{12}C_6$ fructose. Plasma metabolites were measured in the conscious rats at the indicated time points. n = 5–6 per time point and statistical significance was determined by two-way ANOVA and Tukey's test for multiple comparisons. *p < 0.05 for 30 mg/kg, #p < 0.05 for 10 mg/kg, and ^p < 0.05 for 3 mg/kg at the indicated time points. n = 7–8 per group and statistical significance was determined by ANOVA and Bonferroni's test for multiple comparisons. All of the data represent the mean +/− SEM.

To better understand the degree to which PF-06835919 inhibited systemic fructose metabolism, urine and plasma fructose levels were measured in the rats treated with increasing doses of PF-06835919 and administered fructose. In the rats administered vehicle, fructose was undetectable in urine (Figure 2C). Notably, the urine fructose content increased dose-dependently in the rats treated with the KHK inhibitor, with ~10% of the administered fructose recovered in the urine of the rats treated with the highest dose (30 mg/kg) (Figure 2C). In the plasma, a minor increase in fructose was observed in the rats administered vehicle while dose-dependent increases in the plasma fructose levels were observed with PF-06835919 administration (Figure 2D). These data were consistent with observations that ingestion of fructose by mice or people lacking functional KHK leads to increased plasma and urine fructose [24–26].

Following ingestion, fructose also rapidly converts into circulating metabolites including glucose [40,41]. Administering a 50:50 solution of [$^{12}C_6$:$^{13}C_6$] fructose to the rats revealed that the total glucose levels were similar following vehicle or PF-06835919 treatment (Figure 2E). However, a brief drop in plasma glucose levels was observed in all the dose groups possibly due to activation of glucokinase by F1P. Although KHK was inhibited, trace amounts of F1P were still likely produced as inhibition was not capable of full catalytic inactivation. Thus, trace amounts of residual F1P may be sufficient to activate glucokinase [44], as concentrations ranging between 8 and 18 nmol/g liver half maximally activate the kinase in rat hepatocytes [45]. Despite similar levels of total glucose, conversion of [$^{13}C_6$]-fructose carbons into [$^{13}C_3$]-glucose (Figure 2F) and [$^{13}C_6$]-glucose (Figure 2G) dose-dependently decreased following KHK inhibition. Fructose is also generated endogenously by the polyol pathway whereby glucose is first converted into sorbitol and then into fructose [46,47]. Conversion of sorbitol into fructose is reversible, as PF-06835919 dose-dependently increased plasma [$^{13}C_6$]-sorbitol levels (Figure 2H), although this effect was minor. Collectively, these data indicated that PF-06835919 substantially inhibited fructose metabolism in the rats.

3.3. KHK inhibition prevented fructose-induced hyperinsulinemia and hepatic steatosis

To test whether pharmacologic KHK inhibition could blunt fructose-induced metabolic maladaptation, studies with PF-06835919 were conducted in rats fed a diet containing 30% kcal fructose. The rats were randomized into 5 treatment groups, vehicle-treated chow-fed, vehicle-treated fructose-fed, and three fructose-fed groups administered PF-06835919 at 3, 10 and 30 mg/kg/day. These doses were selected to match in vitro KHK enzyme inhibition at IC_{50}, IC_{80}, and $>IC_{80}$ over 24 hrs based on pharmacokinetic/pharmacodynamic modeling. The rats were fed fructose and administered vehicle or PF-06835919 for 7 weeks to understand the durability of KHK inhibition. A detailed pathological end-of-study necropsy revealed that PF-06835919 was well tolerated as no abnormalities were observed (data not shown). The unbound plasma concentration of PF-06835919 was measured on day 16 and confirmed the predicted exposures (Supplemental Figure 2A).

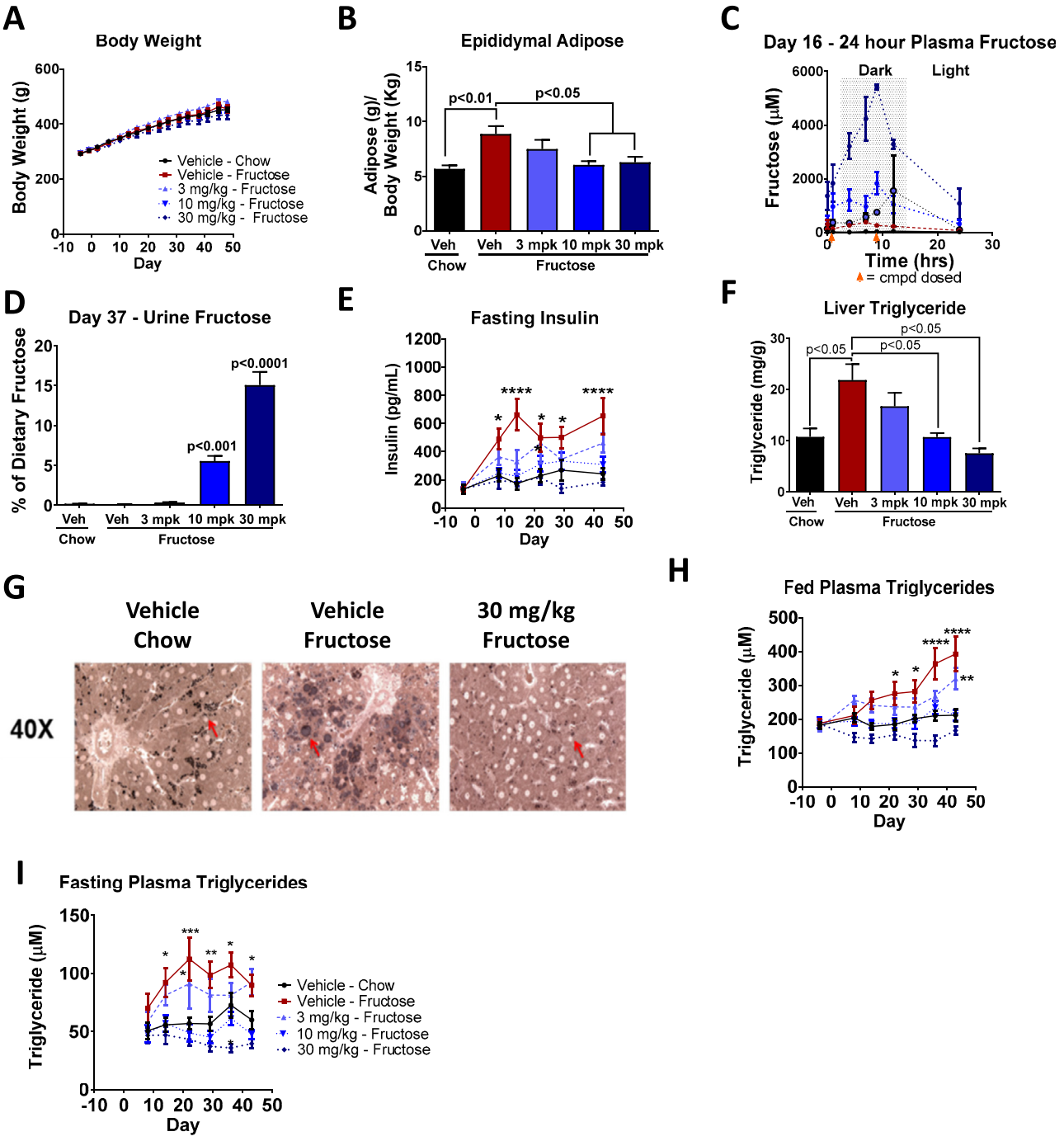

Figure 3: KHK inhibition prevented fructose induced hyperlipidemia, hyperinsulinemia, and steatosis. (A) Body weight of the Sprague Dawley rats fed chow or high-fructose chow with the indicated daily BID dose of PF-06835919 (n = 10/group) for 7 weeks. (B) Perigonadal fat pad mass measured at necropsy (n = 10/group). (C) Day 16 plasma fructose as measured over a 24-hr period in the fructose-fed rats (n = 5/group). (D) Urine fructose content measured from the rats housed in metabolic cages for 24 hrs (n = 10/group). (E) Fasting plasma insulin measured throughout the study (n = 9–10/group). (F) Terminal liver triglycerides (n = 10/group) and (G) osmium PPD-stained histological sample images demonstrating periportal staining. Red arrow = osmium-stained lipid droplet. (H) Weekly fed and (I) fasted plasma triglycerides (n = 10/group). Statistical significance determined by ANOVA and Bonferroni's test for multiple comparisons for B, D, and F. Statistical significance determined by two-way ANOVA and Tukey's test for multiple comparisons of A, C, E, H, and I. *p < 0.05, **p < 0.01, ***p < 0.001, and ****p < 0.0001. All the data represent mean +/− SEM.

Consumption of fructose or treatment with PF-06835919 did not alter body weight (Figure 3A) or weight gain (Supplemental Figure 2B) in the rats. Total caloric intake was also similar between all of the dietary and treatment groups as assessed on day 37 (Supplemental Figure 2C). Interestingly, the increase in epididymal adipose mass caused by fructose feeding in the vehicle-treated rats was prevented by PF-

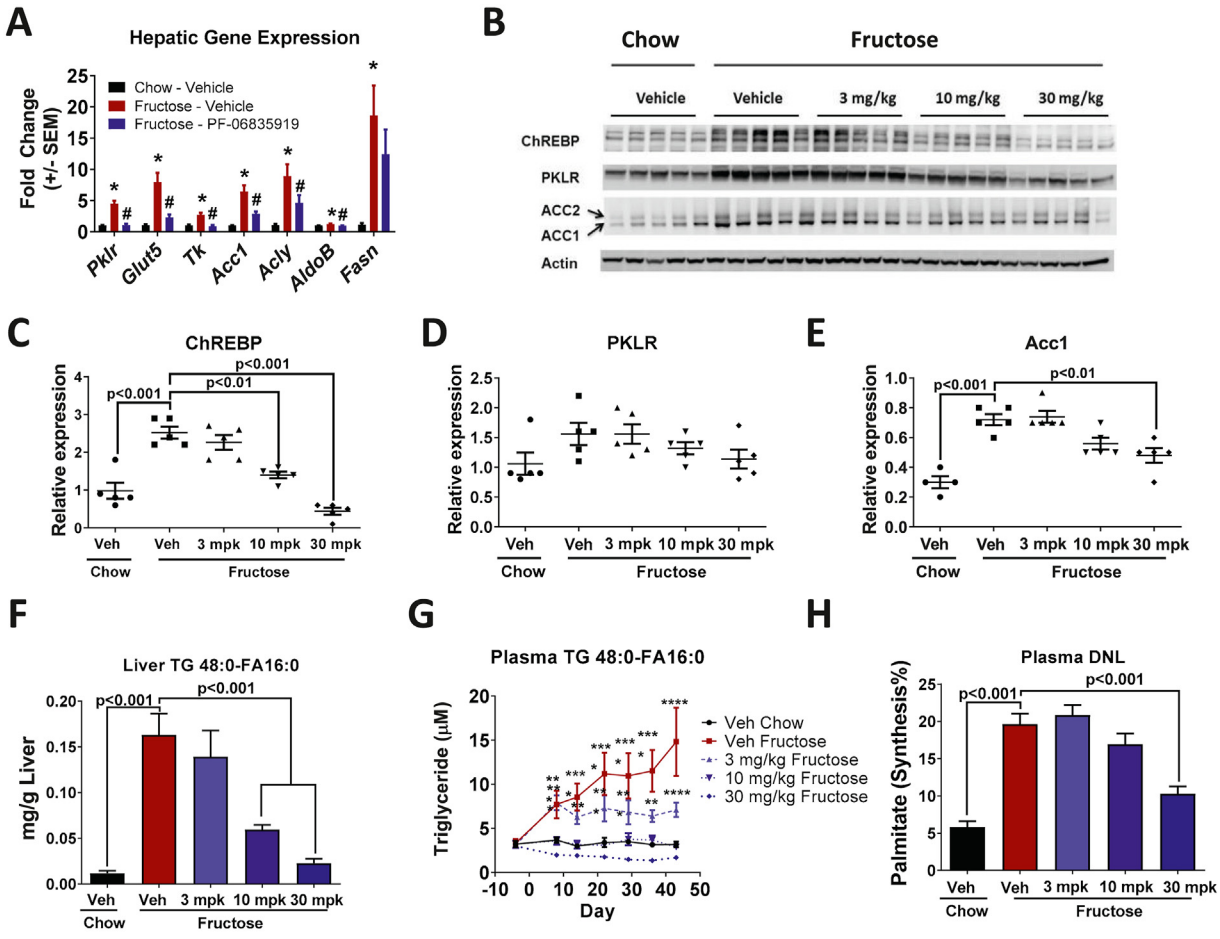

Figure 4: KHK inhibition suppressed ChREBP and DNL in fructose-fed rats. (A) Hepatic gene expression following a 6-hr fast measured in Sprague Dawley rats fed chow or high fructose diet, and treated with vehicle or 30 mg/kg PF-06835919 for 7 days (n = 6/group). Statistical significance determined by ANOVA and Bonferroni's test for multiple comparisons. *p < 0.05 compared to chow and #p < 0.05 compared to vehicle fructose diet. (B–E) Western blotting images and densitometry of hepatic ChREBP, PKLR, and ACC1 normalized to actin (n = 5/group) from the rats fed chow or a fructose diet and treated with PF-06835919 for 7 weeks (n = 5/group). Total terminal liver (F) TG-48:0-FA 16:0 measured by LC-MS/MS from the 7-week study (n = 10/group). Statistical significance determined by ANOVA and Tukey's test for multiple comparisons. (G) Plasma TG-48:0-FA 16:0 measured by LC-MS/MS from weekly plasma samples over the 7-week study (n = 10). Statistical significance was determined by two-way ANOVA and Bonferroni's test for multiple comparisons. (H) D_2O incorporation into plasma palmitate was measured in a separate study with rats fed high fructose diet and treated with the indicated dose of PF-06835919 for two weeks (n = 8/group). Statistical significance determined by ANOVA and Bonferroni's test for multiple comparisons. All the data represent mean +/− SEM. Pyruvate kinase, *Pklr*; solute carrier family 2-facilitated glucose transporter member 5, *Glut5*; triose kinase, *Tk*; acetyl-CoA carboxylase 1, *Acc1*; ATP-citrate synthase, *Acly*; aldolase B, *AldoB;* fatty acid synthase, *Fasn*.

06835919 treatment (Figure 3B). This result was consistent with increased visceral adiposity in humans consuming excess fructose, but not glucose, for 10 weeks [15].

To understand whether prolonged KHK inhibition leads to chronic adaptations in systemic fructose disposal compared to acute inhibition, plasma fructose levels and urine fructose content were measured in the fructose-fed rats administered vehicle or PF-06835919 over 24 hrs. While consumption of fructose negligibly elevated plasma fructose levels in the vehicle-treated rats (Figure 3C and Supplemental Figure 2D), a dose-dependent increase in plasma fructose (Figure 3C), 24-hr fructose AUC (Supplemental Figure 2D), and urine fructose content was observed in the PF-06835919-treated rats (Figure 3D). Approximately 15% of the daily consumed fructose was excreted in the urine of the rats administered the 30 mg/kg dose on day 37 of the study, supporting sustained inhibition of KHK.

We then determined whether features of metabolic dysfunction were observed in the rats fed fructose and whether they could be prevented by KHK inhibition. Consistent with studies in mice and humans [15,18,26], fructose feeding increased fasting insulin levels as early as day 7 in the vehicle-treated rats and was maintained throughout the study, indicative of insulin resistance (Figure 3E). Notably, fasting insulin levels were reduced with increasing doses of PF-06835919 and maintained for the duration of the study (Figure 3E). Despite increased fasting insulin levels, glucose did not change in any of the dietary or PF-06835919-treated groups in the fed state over 24 hrs on day 16 (Supplemental Figure 2E) or upon fasting on day 35 (Supplemental Figure 2F), indicating that, despite their insulin resistance, the fructose-fed rats did not develop overt diabetes.

As genetic deletion of KHK protects mice from fructose-induced hepatic steatosis [26,27], we next sought to determine whether pharmacologic inhibition of KHK could similarly protect the fructose-consuming rats from steatosis. Hepatic triglycerides were increased in the fructose-fed rats administered vehicle compared to that in rats administered chow and dose-dependently decreased by KHK inhibition

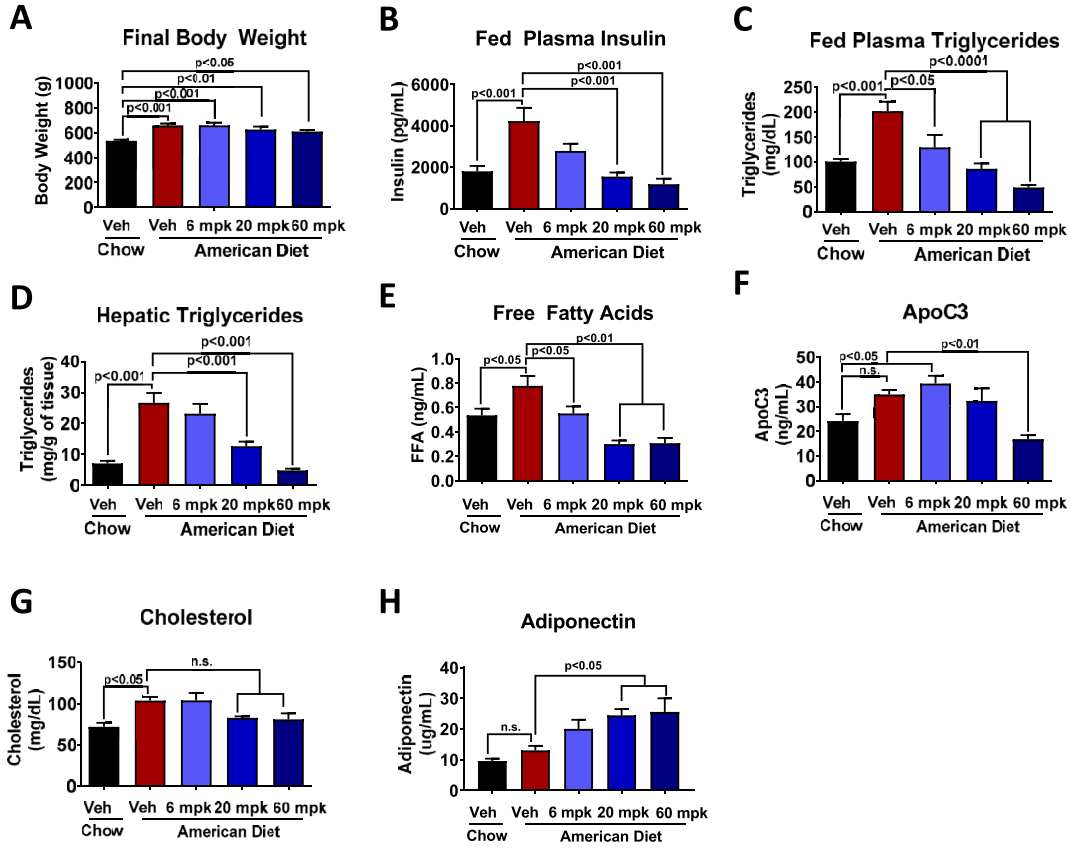

Figure 5: Reversal of hypertriglyceridemia, hyperinsulinemia, and steatosis in the rats fed an "American diet". (A) Final body weights of rats fed an American diet (AD) for 9 weeks and administered vehicle or the indicated dose of PF-06835919 in the final week of the study. (B) Plasma insulin, (C) plasma triglycerides (D), hepatic triglycerides, (E) plasma-free fatty acids, (F) plasma ApoC3, (G) plasma cholesterol, and (H) plasma adiponectin (n = 8/group). Statistical significance determined by ANOVA and Bonferroni's multiple comparison test. All the data represent mean +/− SEM.

(Figure 3F). Histological examination revealed that the majority of steatosis was periportal in the vehicle-treated fructose fed rats and resolved with KHK inhibition (Figure 3G). In addition to promoting steatosis, fructose feeding induces hypertriglyceridemia in mice [26] and humans [15,17,19]. Weekly measurements of fed and fasted plasma triglycerides demonstrated that elevations in the vehicle-treated fructose-fed rats compared to the chow-fed rats were normalized by PF-06835919 in a dose-dependent manner (Figure 3H,I). Thus, fructose feeding promoted steatosis, hyperinsulinemia, and hypertriglyceridemia, which were all completely normalized by KHK inhibition.

As previously discussed, fructose is a potent activator of the transcription factor ChREBP. As expected, hepatic expression of ChREBP target genes *Pklr*, *Glut5*, *Tk*, *Acc1*, *Acly*, *AldoB*, and *Fasn* increased in the fructose-fed rats compared to chow-fed rats after 7 days of feeding (Figure 4A). Treatment with 30 mg/kg of PF-06835919 blunted the expression of these ChREBP target genes in the fructose-fed rats. In the 7-week chronic study, total hepatic ChREBP, PKLR, and ACC1 protein levels also increased in the fructose-fed rats and were dose-dependently reduced by KHK inhibition (Figure 4B–E). Reductions in both mRNA and protein levels of ChREBP target genes demonstrated that KHK inhibition prevented hepatic ChREBP activation by fructose in vivo.

In the rats, fructose feeding increased 16:0, 16:1, 18:0, and 18:1 fatty acid (FA) containing triglyceride (TG) compared to that in the vehicle-treated chow-fed rats consistent with increased DNL (Supplemental Figure 3). Notably, KHK inhibition dose-dependently reduced hepatic levels of these TG species (Supplemental Figure 3). Indeed, a ~10-fold increase in hepatic and ~5-fold increase in plasma TG 48:0-FA16:0 was observed in the fructose-fed rats administered vehicle and was dose-dependently suppressed by KHK inhibition (Figure 4F,G). To verify that the increased abundance of 16:0, 16:1, 18:0, and 18:1 FA in triglycerides was due to increased DNL, the fractional synthesis rate of palmitate was assessed by D_2O incorporation. As shown in Figure 4H, fructose feeding for 2 weeks increased the rate of palmitate synthesis by ~4 fold and this increase was suppressed by treatment with PF-06835919. Together, these data indicate that PF-06835919 blunted metabolic dysfunction in rats caused by fructose consumption.

3.4. PF-06835919 reversed hepatic steatosis and hyperinsulinemia in rats consuming an "American diet"

To understand the potential utility of KHK inhibition in humans consuming a typical Western diet, we tested PF-06835919 using an "American diet" (AD) developed for rodents. The AD was designed so that the fat and fructose kcal % (32% and 7.5% kcal, respectively) mirrored the average macronutrient kcal% consumed by Americans according to the NHANES dietary study [1]. Although the fat and fructose levels in the AD diet were lower than those typically present in high-fat or high-carbohydrate and Western diets used for metabolic

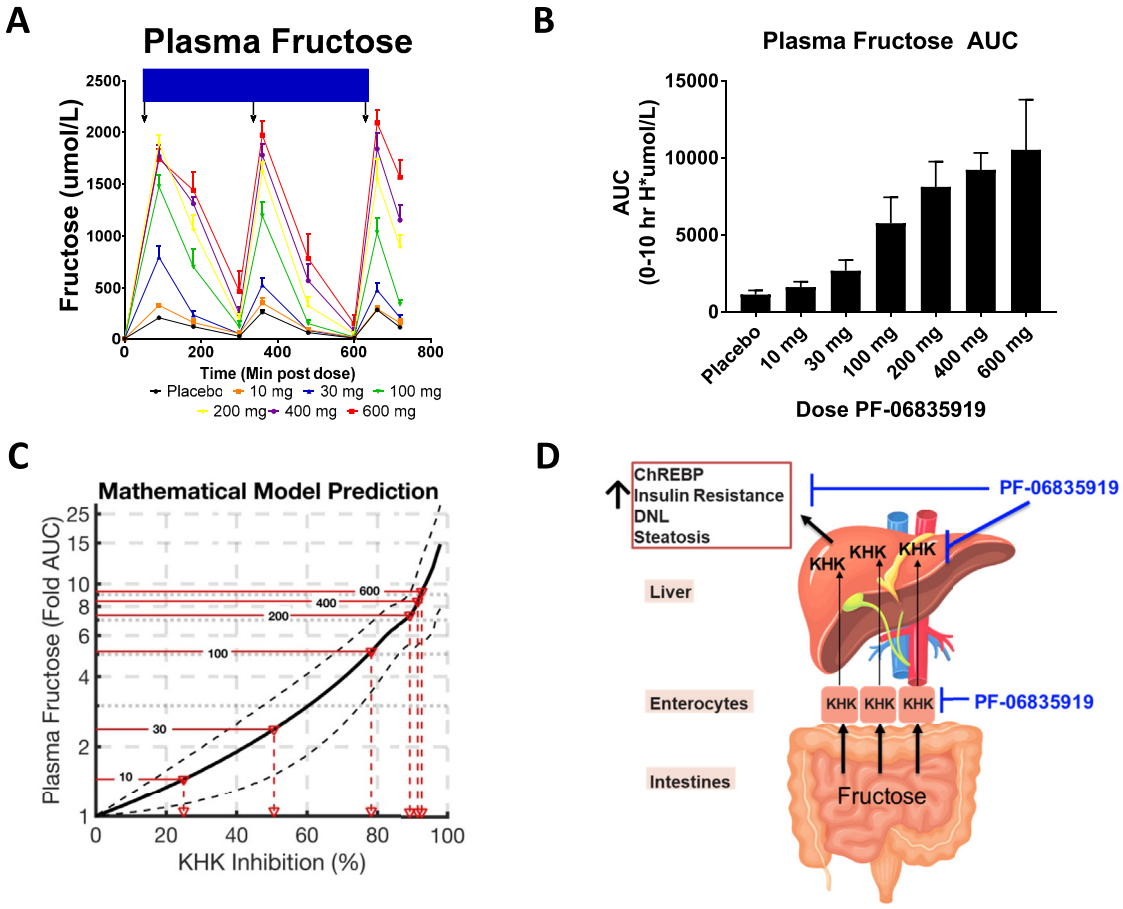

Figure 6: KHK inhibition in humans increased plasma fructose. (A) Plasma fructose levels measured in healthy subjects administered a single dose of PF-06835919. At the indicated time points, the subjects were provided a fructose-sweetened beverage with breakfast, lunch, and dinner. (B) Plasma fructose AUC_{0-10hr} measured in the subjects administered the indicated dose of PF-06835919. (C) Predictive mathematical modeling demonstrating the predicted % KHK inhibition based on the change in AUC_{0-10hr}. (D) Model representing fructose metabolism and how KHK inhibition improves metabolic dysfunction. Ingested fructose is primarily metabolized by enterocytes. Some fructose escapes intestinal metabolism and is metabolized by the liver, promoting ChREBP activation, insulin resistance, DNL, and steatosis. With excessive fructose consumption, hepatic metabolism of fructose metabolism increases due to saturation of intestinal fructose metabolism and/or increased gut permeability, further augmenting ChREBP activation, DNL, insulin resistance, and steatosis. KHK inhibition prevents the metabolism of fructose in enterocytes and hepatocytes, thus reducing ChREBP activation, insulin resistance, DNL, and steatosis (n = 6/group in A and B). All the data represent mean +/− SEM.

studies, the rats consuming AD for only 2 weeks had robust increases in hepatic triglyceride and plasma insulin levels (Supplemental Figure 4A and B), clear hallmarks of metabolic disease.

We next determined whether KHK inhibition could reverse these metabolic disease features. To maximize the diet's effects, we administered ad libitum AD feeding for 8 weeks prior to treatment with vehicle or 6, 20, or 60 mg/kg of PF-06835919 for 1 additional week. The higher doses were selected to ensure robust inhibition of KHK. After 8 weeks of diet, the AD-fed rats weighed significantly more than the chow-fed animals (Supplemental Figure 4C). One week of KHK inhibitor administration did not alter body weights between the vehicle- and inhibitor-treated rats as body weights were similar between all of the AD-fed groups at necropsy (Figure 5A). Plasma insulin and triglycerides, hepatic triglycerides, plasma-free fatty acids, plasma apolipoprotein C3, and total plasma cholesterol were elevated in the AD-fed rats compared to the chow-fed rats and decreased by KHK inhibition, parameters of metabolic disease induced by a diet mirroring the average American diet (Figure 5B–G). Decreases in circulating adiponectin have been reported in both humans and non-human primates fed fructose [48–50]. Surprisingly, adiponectin levels did not differ between chow- and AD-fed rats (Figure 5H), perhaps due to lower fructose levels in the AD or differences between species. However, inhibition of fructose metabolism with PF-06835919 dose-dependently increased adiponectin levels consistent with improved insulin sensitivity.

3.5. A randomized clinical study assessed KHK inhibition in healthy human subjects

As our preclinical studies suggested that inhibition of KHK in human subjects may provide multiple metabolic benefits, a phase 1 single ascending dose study in randomized healthy study participants was conducted to assess the safety, tolerability, and pharmacokinetic properties of PF-06835919: C1061001 (NCT02974374). The study participants were male between the age of 26 and 55 and had mixed ethnic backgrounds with a mean body mass index (BMI) of 26.9 kg/m^2 (Supplemental Table 1). Administration of single oral doses of PF-06835919 was well tolerated in this study, with no serious or severe adverse events reported, and no laboratory abnormalities that were considered clinically significant were observed in participants administered the inhibitor. Dose-dependent increases in plasma PF-

06835919 were observed (Supplemental Table 2) with corresponding dose-dependent increases in plasma fructose and fructose AUC (Figure 6A,B). Consistent with a mathematical model of fructose metabolism used to predict plasma fructose responses to KHK inhibition [39], changes in plasma fructose levels corresponded with increased systemic KHK inhibition following escalating doses, with ~90% or greater inhibition observed in doses above 200 mg (Figure 6C and Supplemental Table 3).

4. DISCUSSION

Excess dietary fructose is associated with increased insulin resistance [15,20], steatosis [16,18,51], and hyperlipidemia [5,15,16,19,21], central features of type 2 diabetes, NAFLD, and cardiovascular disease. Our results suggest that unique properties of fructose metabolism, not simply excess hidden calories, directly promote metabolic dysfunction independent of body weight gain. Considering the global prevalence of dietary fructose and the ever-expanding frequency of metabolic diseases, our studies support pharmacologic inhibition of KHK as a potential therapeutic strategy for addressing common metabolic diseases.

Unlike previous studies using supraphysiologic levels of fructose in rodents to induce features of metabolic syndrome, we demonstrated that high levels of fructose are not required to induce metabolic dysfunction. In rats, the "American diet" induced hyperinsulinemia, hypertriglyceridemia, and steatosis despite only 7.5% of the dietary calories coming from fructose. Hence, real-world amounts of fructose may be sufficient to cause features of metabolic diseases. A publication by Hieronimus et al. [52] demonstrated that glucose and fructose synergize to induce lipoprotein risk factors in humans. Thus, rats fed the "American diet" may better capture physiologic response to fructose than traditional diets containing high fructose alone. Notably, these common features of metabolic disease, including hyperinsulinemia, hypertriglyceridemia, and hepatic steatosis, were reversed by PF-06835919 in rats fed the high-fructose diet or the American diet, suggesting that KHK inhibition may alleviate features of metabolic disease in humans consuming typical diets.

PF-06835919 is a potent systemic inhibitor of KHK as demonstrated by its ability to inhibit the conversion of fructose into F1P in the liver, kidney, and intestines and its downstream metabolites in vivo. A high degree of KHK inhibition is likely necessary due to the high affinity to fructose and capacity for fructose metabolism of KHK [22,26]; thus, this study was enabled by the potency and systemic inhibitory properties of PF-06835919. Importantly, in the phase 1 clinical study, KHK inhibition was demonstrated by dose-dependent increases in plasma fructose levels in the study's participants. This result was consistent with observations in humans and mice lacking KHK, which when administered fructose had similar increases in plasma fructose concentrations [24,26]. Systems modeling determined that KHK was inhibited by over 90% in study participants at the highest doses of PF-06835919. Hence, this is the first demonstration of pharmacologic KHK inhibition in humans.

The adverse metabolic effects of fructose consumption likely result in part from ChREBP-dependent activation of DNL, providing a potential mechanistic basis for the contribution of fructose to metabolic dysfunction. In support, KHK inhibition blunted ChREBP activation and DNL in fructose-fed rats and isolated hepatocytes. The activation of ChREBP is likely mediated by increased hepatic glycolytic metabolites derived from fructose [43,53]. In agreement, reduced ChREBP activation was accompanied by decreased fructose-derived glycolytic intermediates in primary hepatocytes treated with PF-06835919. These results are in line with studies demonstrating protection from fructose-induced DNL, steatosis, hypertriglyceridemia and hyperinsulinemia in fructose-fed rats administered anti-sense oligonucleotides targeting ChREBP [54] and mice with conditional deletion of ChREBP in the intestines or liver [55—57].

Intestinal and hepatic fructose metabolism likely have opposite consequences on metabolic homeostasis (Figure 6D). The primary site of fructose metabolism is the intestine [40]. Metabolism of fructose in the intestines protects the liver from the adverse effects of fructose as conditional deletion of KHK in this tissue exacerbates fructose-induced hepatic lipogenesis and metabolic dysfunction [58—60] Conversely, in a study by Jang et al., intestinal overexpression of KHK prevented fructose-induced DNL [58]. Fructose that escapes intestinal metabolism likely drives hepatic ChREBP activation, DNL, and ensuing metabolic dysfunction. Of note, a report published during the preparation of this manuscript demonstrated that intestinal fructose metabolism decreases intestinal barrier function, increasing "leakiness" and promoting hepatic inflammation [61]. Whether the decrease in intestinal barrier function is driven by fructose metabolism in enterocytes or from bacterial metabolism still needs to be addressed. Hence, understanding the benefits of KHK inhibition beyond the metabolic effects in the liver and the potential impact of KHK inhibition on gut homeostasis and hepatic inflammation will be investigated in the future.

While it should be noted that rodent models may not fully recapitulate all the metabolic effects of fructose consumption and KHK inhibition in humans, the metabolic benefits of KHK inhibition in rats are consistent with the reduced insulin resistance and DNL, hypertriglyceridemia, and steatosis observed in humans with restricted dietary fructose [18,20]. Hence, rats may be an ideal experimental model for studying fructose metabolism and KHK inhibition. Supporting this concept, a manuscript was accepted for publication during the submission of this study demonstrating that PF-06835919 prevented triglyceride accumulation and fibrotic gene expression in human hepatocyte co-cultures and LX-2 cells [29]. The authors also demonstrated that hepatocytes are capable of synthesizing endogenous fructose from glucose via the polyol pathway and that inhibition of the metabolism of this endogenous fructose reduces glucose-induced triglyceride accumulation. While the authors did not test the inhibitor in rodents in their studies, their results in human hepatocyte co-cultures are consistent with the concept that KHK inhibition will reverse fructose-driven triglyceride accumulation.

Of note, the current clinical study was designed to test the safety and tolerability of PF-06835919 and pharmacokinetic relationship of the drug with plasma fructose as a marker of KHK inhibition. As such, the metabolic benefit of KHK inhibition was not assessed in this study. The number of participants was limited and the subjects were healthy, demonstrating no evidence of metabolic disease. The participants received only a single dose of PF-06835919 followed by a $>$6 day washout period between doses of PF-06835919, a treatment paradigm likely insufficient for full metabolic benefit. Ongoing clinical studies with chronic administration of PF-06835919 will test the effects of KHK inhibition on metabolic endpoints (NCT03969719).

A potential concern with pharmacotherapies that increased urinary carbohydrate excretion is a risk of urinary tract infections. In completed clinical studies with PF-06835919, no urinary tract infections were reported in either the placebo or active treatment groups. Furthermore, individuals with loss-of-function mutations in KHK are asymptomatic and increased risk of infection has not been reported despite elevated urinary fructose content [22,24]. Future clinical studies with longer

treatment durations will be necessary to more fully characterize this potential risk.

Despite sustained public awareness about the deleterious metabolic effects of fructose, only slight reductions in fructose consumption over the past few years have been observed. Fructose remains a common additive used in many processed foods, well in excess of dietary guidelines [12,13], accounting for a substantial portion of the dietary calories consumed in the US [13]. The persistent consumption of fructose may result from inadvertent fructose intake due to "hidden" sugar in processed foods. Alternatively, sugar-sweetened beverages continue to be a major source of fructose and may be consumed by those with metabolic risk factors despite physician-directed guidelines. Thus, the prescription of a low-fructose diet may be insufficient for patients who inadvertently consume fructose or choose not to sufficiently change behaviors, leading to exacerbation of metabolic disease. While reducing fructose consumption remains a primary objective for treating obesity and metabolic diseases such as NAFLD, type 2 diabetes, and cardiovascular disease, pharmacological inhibition of fructose metabolism may offer a therapeutic alternative. Future studies with PF-06835919 will enable investigators to assess the role of fructose metabolism in human metabolic disease.

AUTHOR CONTRIBUTIONS

Jemy A. Gutierrez: Conceptualization, investigation, methodology, and writing the original draft. Wei Liu: Conceptualization, investigation, methodology, writing, and review. Sylvie Perez: Investigation, methodology, writing, review, and editing. Gang Xing: Investigation, methodology, writing, review, and editing. Gabriele Sonnenberg: Investigation, methodology, writing, review, and editing. Kou Kou: Investigation, methodology, writing, review, and editing. Matt Blatnik: Investigation, methodology, writing, review, and editing. Richard Allen: Methodology, software, writing, review, and editing. Yan Weng: Methodology, writing, review, and editing. Nicholas B. Vera: Investigation, writing, review, and editing. Kristin Chidsey: Investigation, methodology, writing, review, and editing. Arthur Bergman: Methodology, writing, review, and editing. Veena Somayaji: Methodology, formal analysis, writing, review, and editing. Collin Crowley: Investigation, writing, review, and editing. Michelle F. Clasquin: methodology, writing, review, and editing. Anu Nigam: Investigation and methodology. Derek M. Erion: Conceptualization and investigation. Melissa A. Fulham: Investigation, writing, review, and editing. Trenton T. Ross: Investigation, methodology, writing, review, and editing. William P. Esler: Conceptualization, writing, review, and editing. Thomas V. Magee: Conceptualization, writing, review, and editing. Jeffrey A. Pfefferkorn: Conceptualization, writing, review, and editing. Kendra K. Bence: Conceptualization, writing, review, and editing. Morris J. Birnbaum: Conceptualization, writing, review, and editing. Gregory J. Tesz: Conceptualization, investigation, methodology, supervision, and writing original draft.

ACKNOWLEDGMENTS

We thank the healthy adults who participated in the studies, the investigators, and the site coordinators who helped conduct the clinical study. We are grateful to Stephanie-An Lyle for help with preparing the CONSORT flow chart and diagram. We also thank John Meissen for help with the metabolomics, Saswata Talukdar for help in conducting the experiments and enthusiastic discussions about fructose metabolism, and Leslie King for help in drafting and preparing this manuscript. We also acknowledge Tim Rolph for supporting the initial work. The study presented herein was funded by Pfizer, New York, NY, USA.

CONFLICTS OF INTEREST

All of the authors are either current or former employees of Pfizer and may be Pfizer shareholders.

APPENDIX A. SUPPLEMENTARY DATA

Supplementary data to this article can be found online at https://doi.org/10.1016/j.molmet.2021.101196.

REFERENCES

[1] Marriott, B.P., Olsho, L., Hadden, L., Connor, P., 2010. Intake of added sugars and selected nutrients in the United States, national health and nutrition examination survey (NHANES) 2003-2006. Critical Reviews in Food Science and Nutrition 50(3):228—258.

[2] Schulze, M.B., Manson, J.E., Ludwig, D.S., Colditz, G.A., Stampfer, M.J., Willett, W.C., et al., 2004. Sugar-sweetened beverages, weight gain, and incidence of type 2 diabetes in young and middle-aged women. Journal of the American Medical Association 292(8):927—934.

[3] Palmer, J.R., Boggs, D.A., Krishnan, S., Hu, F.B., Singer, M., Rosenberg, L., 2008. Sugar-sweetened beverages and incidence of type 2 diabetes mellitus in African American women. Archives of Internal Medicine 168(14):1487—1492.

[4] Yang, Q., Zhang, Z., Gregg, E.W., Flanders, W.D., Merritt, R., Hu, F.B., 2014. Added sugar intake and cardiovascular diseases mortality among US adults. JAMA Internal Medicine 174(4):516—524.

[5] Dhingra, R., Sullivan, L., Jacques, P.F., Wang, T.J., Fox, C.S., Meigs, J.B., et al., 2007. Soft drink consumption and risk of developing cardiometabolic risk factors and the metabolic syndrome in middle-aged adults in the community. Circulation 116(5):480—488.

[6] Despland, C., Walther, B., Kast, C., Campos, V., Rey, V., Stefanoni, N., et al., 2017. A randomized-controlled clinical trial of high fructose diets from either Robinia honey or free fructose and glucose in healthy normal weight males. Clinical Nutrition ESPEN 19:16—22.

[7] Abdelmalek, M.F., Lazo, M., Horska, A., Bonekamp, S., Lipkin, E.W., Balasubramanyam, A., et al., 2012. Higher dietary fructose is associated with impaired hepatic adenosine triphosphate homeostasis in obese individuals with type 2 diabetes. Hepatology 56(3):952—960.

[8] Abid, A., Taha, O., Nseir, W., Farah, R., Grosovski, M., Assy, N., 2009. Soft drink consumption is associated with fatty liver disease independent of metabolic syndrome. Journal of Hepatology 51(5):918—924.

[9] Assy, N., Nasser, G., Kamayse, I., Nseir, W., Beniashvili, Z., Djibre, A., et al., 2008. Soft drink consumption linked with fatty liver in the absence of traditional risk factors. Canadian Journal of Gastroenterology 22(10):811—816.

[10] Ma, J., Fox, C.S., Jacques, P.F., Speliotes, E.K., Hoffmann, U., Smith, C.E., et al., 2015. Sugar-sweetened beverage, diet soda, and fatty liver disease in the Framingham Heart Study cohorts. Journal of Hepatology 63(2):462—469.

[11] Abdelmalek, M.F., Suzuki, A., Guy, C., Unalp-Arida, A., Colvin, R., Johnson, R.J., et al., 2010. Increased fructose consumption is associated with fibrosis severity in patients with nonalcoholic fatty liver disease. Hepatology 51(6):1961—1971.

[12] Mohan, A., 2015. WHO recommends reducing intake of 'free sugars' by adults and children. The National Medical Journal of India 28(3):165.

[13] Vos, M.B., 2014. Nutrition, nonalcoholic fatty liver disease and the microbiome: recent progress in the field. Current Opinion in Lipidology 25(1):61—66.

[14] Cozma, A.I., Sievenpiper, J.L., 2014. The role of fructose, sucrose and high-fructose corn syrup in diabetes. European Endocrinology 10(1):51—60.

[15] Stanhope, K.L., Schwarz, J.M., Keim, N.L., Griffen, S.C., Bremer, A.A., Graham, J.L., et al., 2009. Consuming fructose-sweetened, not glucose-sweetened, beverages increases visceral adiposity and lipids and decreases insulin sensitivity in overweight/obese humans. Journal of Clinical Investigation 119(5):1322–1334.

[16] Taskinen, M.R., Soderlund, S., Bogl, L.H., Hakkarainen, A., Matikainen, N., Pietilainen, K.H., et al., 2017. Adverse effects of fructose on cardiometabolic risk factors and hepatic lipid metabolism in subjects with abdominal obesity. Journal of Internal Medicine 282(2):187–201.

[17] Swarbrick, M.M., Stanhope, K.L., Elliott, S.S., Graham, J.L., Krauss, R.M., Christiansen, M.P., et al., 2008. Consumption of fructose-sweetened beverages for 10 weeks increases postprandial triacylglycerol and apolipoprotein-B concentrations in overweight and obese women. British Journal of Nutrition 100(5):947–952.

[18] Schwarz, J.M., Noworolski, S.M., Erkin-Cakmak, A., Korn, N.J., Wen, M.J., Tai, V.W., et al., 2017. Effects of dietary fructose restriction on liver fat, de novo lipogenesis, and insulin kinetics in children with obesity. Gastroenterology 153(3):743–752.

[19] Stanhope, K.L., Medici, V., Bremer, A.A., Lee, V., Lam, H.D., Nunez, M.V., et al., 2015. A dose-response study of consuming high-fructose corn syrup-sweetened beverages on lipid/lipoprotein risk factors for cardiovascular disease in young adults. American Journal of Clinical Nutrition 101(6):1144–1154.

[20] Lustig, R.H., Mulligan, K., Noworolski, S.M., Tai, V.W., Wen, M.J., Erkin-Cakmak, A., et al., 2016. Isocaloric fructose restriction and metabolic improvement in children with obesity and metabolic syndrome. Obesity 24(2):453–460.

[21] Gugliucci, A., Lustig, R.H., Caccavello, R., Erkin-Cakmak, A., Noworolski, S.M., Tai, V.W., et al., 2016. Short-term isocaloric fructose restriction lowers apoC-III levels and yields less atherogenic lipoprotein profiles in children with obesity and metabolic syndrome. Atherosclerosis 253:171–177.

[22] Bonthron, D.T., Brady, N., Donaldson, I.A., Steinmann, B., 1994. Molecular basis of essential fructosuria: molecular cloning and mutational analysis of human ketohexokinase (fructokinase). Human Molecular Genetics 3(9):1627–1631.

[23] Diggle, C.P., Shires, M., Leitch, D., Brooke, D., Carr, I.M., Markham, A.F., et al., 2009. Ketohexokinase: expression and localization of the principal fructose-metabolizing enzyme. Journal of Histochemistry and Cytochemistry 57(8):763–774.

[24] Sachs, B., Sternfeld, L., Kraus, G., 1942. Essential fructosuria: its pathophysiology. American Journal of Diseases of Children 63:252–269.

[25] Laron, Z., 1961. Essential benign fructosuria. Archives of Disease in Childhood 36:273–277.

[26] Ishimoto, T., Lanaspa, M.A., Le, M.T., Garcia, G.E., Diggle, C.P., Maclean, P.S., et al., 2012. Opposing effects of fructokinase C and A isoforms on fructose-induced metabolic syndrome in mice. Proceedings of the National Academy of Sciences of the U S A 109(11):4320–4325.

[27] Ishimoto, T., Lanaspa, M.A., Rivard, C.J., Roncal-Jimenez, C.A., Orlicky, D.J., Cicerchi, C., et al., 2013. High-fat and high-sucrose (western) diet induces steatohepatitis that is dependent on fructokinase. Hepatology 58(5):1632–1643.

[28] Softic, S., Gupta, M.K., Wang, G.X., Fujisaka, S., O'Neill, B.T., Rao, T.N., et al., 2018. Divergent effects of glucose and fructose on hepatic lipogenesis and insulin signaling. Journal of Clinical Investigation 128(3):1199.

[29] Shepherd, E.L., Saborano, R., Northall, E., Matsuda, K., Ogino, H., Yashiro, H., et al., 2021. Ketohexokinase inhibition improves NASH by reducing fructose-induced steatosis and fibrogenesis. JHEP Reports 3(2):100217.

[30] Futatsugi, K., Smith, A.C., Tu, M., Raymer, B., Ahn, K., Coffey, S.B., et al., 2020. Discovery of PF-06835919: a potent inhibitor of ketohexokinase (KHK) for the treatment of metabolic disorders driven by the overconsumption of fructose. Journal of Medicinal Chemistry 63(22):13546–13560.

[31] Meissen, J.K., Pirman, D.A., Wan, M., Miller, E., Jatkar, A., Miller, R., et al., 2016. Phenotyping hepatocellular metabolism using uniformly labeled carbon-13 molecular probes and LC-HRMS stable isotope tracing. Analytical Biochemistry 508:129–137.

[32] Shirai, N., Geoly, F.J., Bobrowski, W.F., Okerberg, C., 2016. The application of paraphenylenediamine staining for assessment of phospholipidosis. Toxicologic Pathology 44(8):1160–1165.

[33] Bligh, E.G., Dyer, W.J., 1959. A rapid method of total lipid extraction and purification. Canadian Journal of Biochemistry and Physiology 37(8):911–917.

[34] Morrison, W.R., Smith, L.M., 1964. Preparation of fatty acid methyl esters and dimethylacetals from lipids with boron fluoride–methanol. The Journal of Lipid Research 5:600–608.

[35] Lee, W.N., Bassilian, S., Ajie, H.O., Schoeller, D.A., Edmond, J., Bergner, E.A., et al., 1994. In vivo measurement of fatty acids and cholesterol synthesis using D2O and mass isotopomer analysis. American Journal of Physiology 266(5 Pt 1):E699–E708.

[36] Guo, Z.K., Cella, L.K., Baum, C., Ravussin, E., Schoeller, D.A., 2000. De novo lipogenesis in adipose tissue of lean and obese women: application of deuterated water and isotope ratio mass spectrometry. International Journal of Obesity and Related Metabolic Disorders 24(7):932–937.

[37] Elhamdy, A., Christie, W., 1993. Separation of non-polar lipids by high performance liquid chromatography on a cyanopropyl column. Journal of High Resolution Chromatography 16:55–57.

[38] Kaluzny, M.A., Duncan, L.A., Merritt, M.V., Epps, D.E., 1985. Rapid separation of lipid classes in high yield and purity using bonded phase columns. The Journal of Lipid Research 26(1):135–140.

[39] Allen, R.J., Musante, C.J., 2018. A mathematical analysis of adaptations to the metabolic fate of fructose in essential fructosuria subjects. American Journal of Physiology. Endocrinology and Metabolism 315(3):E394–E403.

[40] Jang, C., Hui, S., Lu, W., Cowan, A.J., Morscher, R.J., Lee, G., et al., 2018. The small intestine converts dietary fructose into glucose and organic acids. Cell Metabolism 27(2):351–361 e353.

[41] Sun, S.Z., Empie, M.W., 2012. Fructose metabolism in humans - what isotopic tracer studies tell us. Nutrition and Metabolism 9(1):89.

[42] Iizuka, K., Bruick, R.K., Liang, G., Horton, J.D., Uyeda, K., 2004. Deficiency of carbohydrate response element-binding protein (ChREBP) reduces lipogenesis as well as glycolysis. Proceedings of the National Academy of Sciences of the U S A 101(19):7281–7286.

[43] Dentin, R., Tomas-Cobos, L., Foufelle, F., Leopold, J., Girard, J., Postic, C., et al., 2012. Glucose 6-phosphate, rather than xylulose 5-phosphate, is required for the activation of ChREBP in response to glucose in the liver. Journal of Hepatology 56(1):199–209.

[44] Matschinsky, F.M., 2009. Assessing the potential of glucokinase activators in diabetes therapy. Nature Reviews Drug Discovery 8(5):399–416.

[45] Davies, D.R., Detheux, M., Van Schaftingen, E., 1990. Fructose 1-phosphate and the regulation of glucokinase activity in isolated hepatocytes. European Journal of Biochemistry 192(2):283–289.

[46] Lanaspa, M.A., Ishimoto, T., Li, N., Cicerchi, C., Orlicky, D.J., Ruzycki, P., et al., 2013. Endogenous fructose production and metabolism in the liver contributes to the development of metabolic syndrome. Nature Communications 4:2434.

[47] Lanaspa, M.A., Ishimoto, T., Cicerchi, C., Tamura, Y., Roncal-Jimenez, C.A., Chen, W., et al., 2014. Endogenous fructose production and fructokinase activation mediate renal injury in diabetic nephropathy. Journal of the American Society of Nephrology 25(11):2526–2538.

[48] Bremer, A.A., Stanhope, K.L., Graham, J.L., Cummings, B.P., Wang, W., Saville, B.R., et al., 2011. Fructose-fed rhesus monkeys: a nonhuman primate model of insulin resistance, metabolic syndrome, and type 2 diabetes. Clinical Translational Science(4):243–252.

[49] Butler, A.A., Graham, J.L., Stanhope, K.L., Wong, S., King, S., Bremer, A.A., et al., 2020. Role of angiopoietin-like protein 3 in sugar-induced dyslipidemia in rhesus macaques: suppression by fish oil or RNAi. The Journal of Lipid Research 61(3):376–386.

[50] Rezvani, R., Cianflone, K., McGahan, J.P., Berglund, L., Bremer, A.A., Keim, N.L., et al., 2013. Effects of sugar-sweetened beverages on plasma acylation stimulating protein, leptin and adiponectin: relationships with metabolic outcomes. Obesity 21(12):2471—2480.

[51] Schwarz, J.M., Noworolski, S.M., Wen, M.J., Dyachenko, A., Prior, J.L., Weinberg, M.E., et al., 2015. Effect of a high-fructose weight-maintaining diet on lipogenesis and liver fat. The Journal of Cinical Endocrinology and Metabolism 100(6):2434—2442.

[52] Hieronimus, B., Stanhope, K.L., 2020. Dietary fructose and dyslipidemia: new mechanisms involving apolipoprotein CIII. Current Opinion in Lipidology 31(1): 20—26.

[53] Abdul-Wahed, A., Guilmeau, S., Postic, C., 2017. Sweet sixteenth for ChREBP: established roles and future goals. Cell Metabolism 26(2):324—341.

[54] Erion, D.M., Popov, V., Hsiao, J.J., Vatner, D., Mitchell, K., Yonemitsu, S., et al., 2013. The role of the carbohydrate response element-binding protein in male fructose-fed rats. Endocrinology 154(1):36—44.

[55] Herman, M.A., Samuel, V.T., 2016. The sweet path to metabolic demise: fructose and lipid synthesis. Trends in Endocrinology and Metabolism 27(10):719—730.

[56] Kim, M., Astapova II, , Flier, S.N., Hannou, S.A., Doridot, L., Sargsyan, A., et al., 2017. Intestinal, but not hepatic, ChREBP is required for fructose tolerance. JCI Insight 2(24).

[57] Kim, M.S., Krawczyk, S.A., Doridot, L., Fowler, A.J., Wang, J.X., Trauger, S.A., et al., 2016. ChREBP regulates fructose-induced glucose production independently of insulin signaling. Journal of Clinical Investigation 126(11):4372—4386.

[58] Jang, C., Wada, S., Yang, S., Gosis, B., Zeng, X., Zhang, Z., et al., 2020. The small intestine shields the liver from fructose-induced steatosis. Nature Metabolism 2(7):586—593.

[59] Andres-Hernando, A., Orlicky, D.J., Kuwabara, M., Ishimoto, T., Nakagawa, T., Johnson, R.J., et al., 2020. Deletion of fructokinase in the liver or in the intestine reveals differential effects on sugar-induced metabolic dysfunction. Cell Metabolism 32(1):117—127 e113.

[60] Tesz, G.J., Bence, K.K., 2020. Finding the sweet spot: parsing tissue-specific contributions of fructose metabolism. Cell Metabolism 32(1):6—8.

[61] Todoric, J., Di Caro, G., Reibe, S., Henstridge, D.C., Green, C.R., Vrbanac, A., et al., 2020. Fructose stimulated de novo lipogenesis is promoted by inflammation. Nature Metabolism 2:1034—1045.

